ELSEVIER

Marine Geology xx (2004) xxx–xxx

MARINE GEOLOGY
INTERNATIONAL JOURNAL OF MARINE GEOLOGY, GEOCHEMISTRY AND GEOPHYSICS

www.elsevier.com/locate/margeo

Classification of the Australian continental shelf based on predicted sediment threshold exceedance from tidal currents and swell waves

R. Porter-Smith[a,*], P.T. Harris[a,1], O. Anderson[b], R. Coleman[c,d,2], D. Greenslade[e,3], C.J. Jenkins[f,4]

[a] *Geoscience Australia, GPO Box 378, Canberra ACT, 2601, Australia*
[b] *Kort and Matrikelstyrelsen, Geodetic Division, Rentemestervej 8, DK-2400 Copenhagen NV, Denmark*
[c] *Department of Surveying and Spatial Information Science, University of Tasmania, GPO Box 252-76, Hobart, Tasmania 7001, Australia*
[d] *CSIRO, Division of Marine Research, GPO Box 1538, Hobart, Tasmania 7001 Australia*
[e] *Bureau of Meteorology Research Centre, Melbourne, Victoria 3001, Australia*
[f] *Institute of Arctic and Alpine, University of Colorado, Boulder, CO, USA*

Received 25 September 2001; accepted 28 May 2004

Abstract

Estimates of significant wave height and period, together with tidal current speed over a semi-lunar cycle, were used to predict the area on the Australian continental shelf over which unconsolidated sediment was mobilised (threshold exceedance). These sediment-entraining processes were examined independently to quantify their relative importance on the continental shelf. Using observed grain size data, mobilisation from swell waves occurred on ~31% and tidal currents on ~41% of the continental shelf. Swell wave energy is sufficient to mobilise fine sand (0.1 mm diameter) to a water depth of 142 m on the Otway Shelf near the western entrance to Bass Strait. Tidal currents in King Sound (northwest shelf) are capable of mobilising large areas of medium sand (0.35 mm diameter) 100% of the time. Superimposing the distribution of threshold exceedance by wave and tidal currents indicates that there are areas on the shelf where either wave-induced or tidal currents dominate, some areas where waves and tides are of relatively equal importance and still other areas where neither is significant. We define six shelf regions of relative wave and tidal energy: zero (no-mobility); waves-only, wave-dominated, mixed, tide-dominated and tides-only. Our results provide a predictive, process-based understanding of the shelf sedimentary system that has applications to marine engineering projects and to regional studies of pollution dispersal and accumulation where significant shelf sediment mobilisation is a factor.

Keywords: sediment; mobility; classification; habitat; regionalisation; Australia

* Corresponding author. Antarctic CRC, University of Tasmania, GPO Box 252-80, Hobart TAS. 7001, Australia. Fax: +61-3-6226-2973.
E-mail addresses: r.smith@utas.edu.au (R. Porter-Smith), peter.harris@ga.gov.au (P.T. Harris), oa@kms.dk (O. Anderson), richard.coleman@utas.edu.au (R. Coleman), dag@bom.gov.au (D. Greenslade), chris.jenkins@colorado.edu (C.J. Jenkins).
[1] Fax: +61-3-6226-2973.
[2] Fax: +61-3-6224-0282.
[3] Fax: +61-3-9669-4660.
[4] Fax: +1-303-492-6388.

0025-3227/$ - see front matter © 2004 Elsevier B.V. All rights reserved.
doi:10.1016/j.margeo.2004.05.031

1. Introduction

An unanswered question in continental shelf sediment research is "What percentage of the Earth's continental shelves are subject to hydrodynamic processes strong enough to mobilise the bed sediment (Swift and Thorne, 1991)?" Although it has been suggested that about 80% of the world's shelves are dominated by storm-waves, 17% by tidal currents and 3% by ocean–current interactions (Walker, 1984; Swift et al., 1986), there is currently no published quantitative analysis of continental shelves to determine the spatial distribution of dominant sediment transport processes. The main limitation has been the practical difficulties involved in collecting enough data over the shelf. In a first attempt at quantifying the influence of the global wave climate on sediment mobility, Harris and Coleman (1998) used wave data generated by a global climate model. They found that the wave climate was capable of mobilising 0.1 mm diameter quartz sand over 41.6% of the earth's continental shelves on at least one occasion during a 3-year period from July 1992 to July 1995.

For the Australian continental shelf, Harris (1995) proposed a classification based on the relative influence of storms (including tropical cyclones), swell waves, tidal currents and intruding ocean currents. According to this scheme (Fig. 1), the Australian shelf may be subdivided into areas where storm processes dominate in the mobilisation of sediments (82% of the shelf), where tidal currents dominate (17.4%), and where intruding ocean currents dominate (< 1%).

The aims of the present study are twofold. Firstly, our aim is to extend the work of Harris and Coleman (1998) for the Australian region by incorporating a finer resolution wave climatology data set, together with a similar spatial resolution shelf tide model. This will allow a more detailed assessment of the relative spatial distribution of wave- and tide-dominated portions of the Australian continental shelf. Secondly, our aim is to use observed sediment data to examine the relationship between mean grain size (D_{50}) and current velocity (U_{max}) produced from tides and waves. It is acknowledged that other processes such as continental shelf waves have the potential to mobilise sediment on the continental shelf (Freeland et al., 1986), however for this study it has been decided to concentrate on the two main processes of tidal currents and swell waves.

1.1. Shelves dominated by storms

Storm-dominated regions of the Australian shelf may experience one or several storm events per year which cause sediment transporting flows. Currents produced during the passage of storm events control the erosion and transport of unconsolidated sediment over an estimated 82% of the Australian shelf surface area (Harris, 1995). Storms occur in the form of tropical cyclones and temperate low-pressure systems. The energy expended and the amount of sediment transported during one storm event may equal many months (or years) of fair-weather transport (e.g. Swift and Thorne, 1991). Even on highly dynamic, tidally influenced shelves, the effect of a storm event is to initiate sediment movement at even greater water depths and at greater rates in shallower depths than is experienced under fair-weather conditions.

Significant wave height data obtained from satellite altimeters illustrates that, although significant wave heights are less than 1.5 m for 50–70% of the time in northern Australia, they are larger than 3.5 m for 30–50% of the time along much of the southern Australia shelf (McMillan, 1982; Fig. 1). Storm events influence not only the initiation of sediment movement, but also the deposition of sediment. Examples of studies in Australia which have documented the development of shelf storm deposits include those of the Rottnest Shelf (Collins, 1988), the Lacepede Shelf coast (James et al., 1992), the New South Wales Shelf (Davies, 1979) and Gippsland Shelf (Black and Oldman, 1999). In these locations (Fig. 2), long-period swell waves cause nearly continuous reworking of sediment on the inner shelf, winnowing away fine grains and leaving a sorted, sandy deposit. On the New South Wales shelf, mud is deposited in water depths of between 60 and 130 m (Gordon and Hoffman, 1986) and on the higher energy Lacepede shelf mud is deposited below 140 m (James et al., 1992). On the southern parts of Australia's shelf, the sediment is arranged in zones parallel to the coast (James et al., 1992), reflecting the dominance of ocean swell waves and storms (Fig. 1).

Tropical cyclones are the cause of storm events in much of northern Australia (Lourensz, 1981; Fig. 1). The sections of the northern shelf most frequently

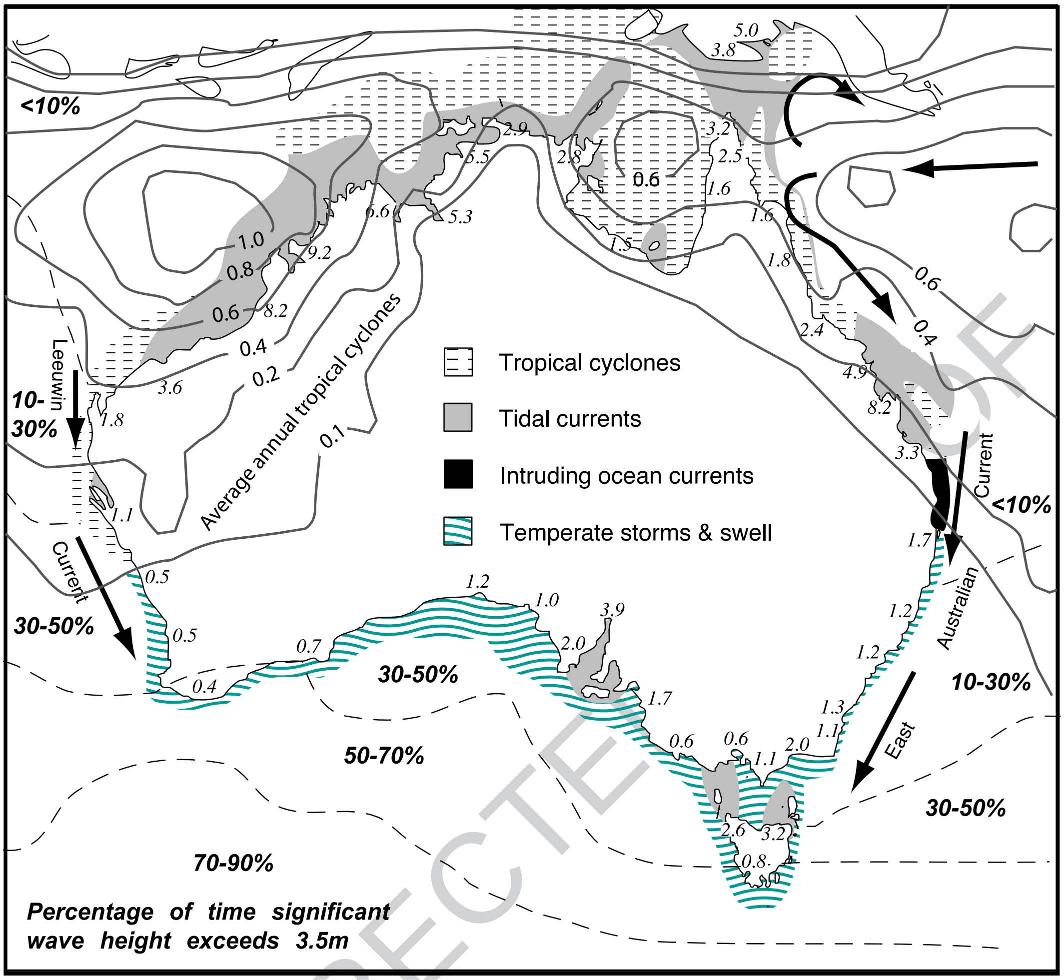

Fig. 1. Division of the Australian shelf (after Harris, 1995) into regions in which sediment transport is caused mainly by tidal currents (17.4% of the shelf area), currents derived from tropical cyclones (53.8%), ocean swell and storm generated currents (28.2%) and intruding ocean currents (0.6%). Contours representing tropical cyclone frequency are from the Bureau of Meteorology (http://www.bom.gov.au/climate/averages/climatology/tropical_cyclones/tropical_cycl.shtml) and contours for significant wave height percentage exceedence are from McMillan (1982). Mean spring tidal ranges indicated along the coastline are derived from the Australian National Tide Tables. The location and direction of flow of major ocean currents are indicated.

affected by cyclones include the North West Shelf, Gulf of Carpentaria and the Great Barrier Reef. Information on the frequency of tropical cyclones can be found on the Bureau of Meteorology's site http://www.bom.gov.au/climate/averages/climatology/tropical_cyclones/tropical_cycl.shtml.

These shelf areas experience generally small (< 1.5 m significant wave height) ocean swell waves (Fig. 1). Tropical cyclones induce strong currents, which erode and transport sediment over a wide area (Gagan et al., 1990). Current meter measurements, obtained in the Gulf of Carpentaria during one tropical cyclone, recorded near-bed currents that attained hourly speeds up to six times larger than during fair-weather conditions (Church and Forbes, 1983). In the Great Barrier Reef, Cyclone Winfred produced a mixed terrigenous-carbonate storm layer averaging 6.9 cm thick on the middle shelf, and transported sediment alongshore and northward a minimum distance of 15 km (Gagan et al., 1990).

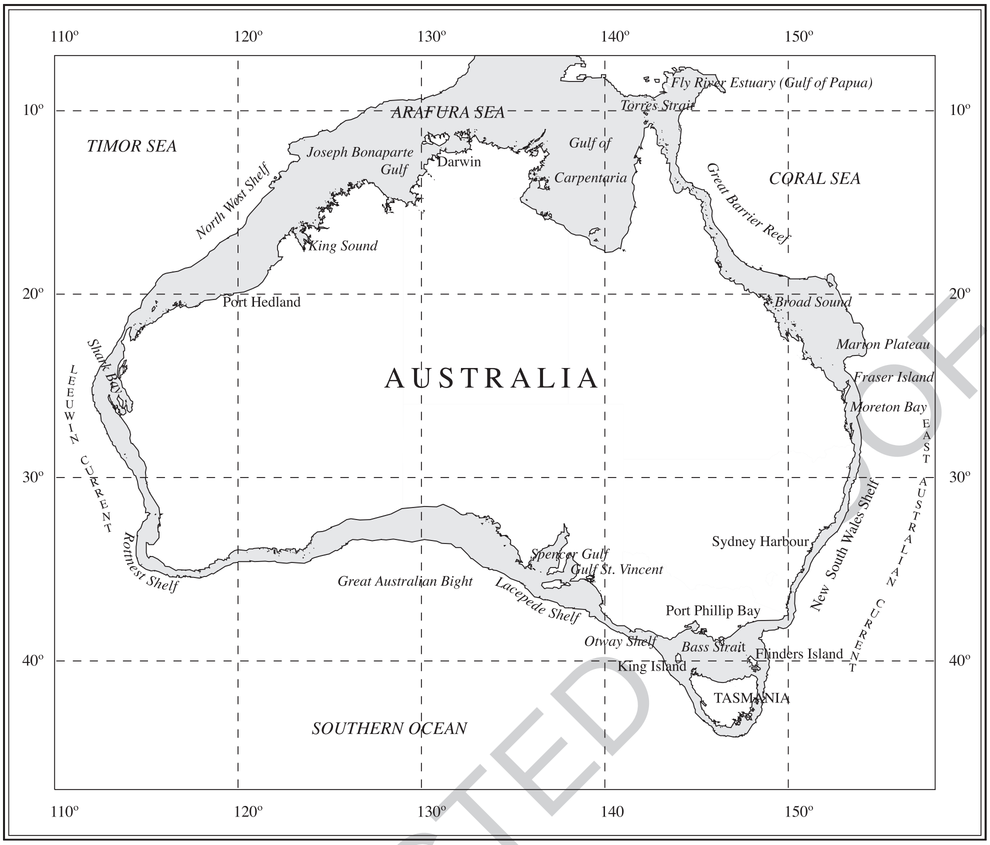

Fig. 2. Map of Australia showing geographic locations cited in the text.

Modelling studies by Hearn and Holloway (1990) on the North West Shelf have shown that, under the influence of tropical cyclones, strong westward-flowing coastal and inner shelf currents are established between the eye of the cyclone and the coast. Such cyclone-induced currents are clearly a significant factor affecting sediment movement on cyclone-dominated shelves, but they may also influence the long-term (net) sediment movement on some otherwise tidally dominated sections of the shelf (Harris, 1995).

1.2. Shelves dominated by tides

Tidally dominated, macrotidal shelves occur where the mean spring tidal range measured along the coast exceeds 4 m (Walker, 1984). Around Australia, tidal ranges >4 m occur along the north west shelf between Port Hedland and Darwin (Fig. 2), and attain 12.5 m in King Sound (Figs. 1 and 2). The southern Great Barrier Reef platform is also macrotidal, with a maximum tidal range of 8.2 m in Broad Sound (Fig. 2). In the Fly River Delta (Gulf of Papua; Fig. 2) tidal ranges are up to 5 m (Harris et al., 1993). Tidal currents are also an important sand transporting mechanism in mesotidal (2–4 m tidal range) regions such as Torres Strait, Bass Strait and Moreton Bay (Fig. 2). Tidal currents are capable of controlling sand transport in microtidal regions (tidal range <2 m) in restricted cases, where coastal geometry affords shelter from ocean-generated swell and wind-driven currents (Harris, 1994). Such is the case in many bays (e.g. Shark Bay), the approaches to some major ports (e.g. Port Phillip Bay, Melbourne) and in partly enclosed Gulfs (e.g. Spencer Gulf, Gulf St. Vincent and the Gulf of Carpentaria). Tidal currents are accelerated as they flow over and between shelf edge barrier reefs, thus sediment transport is affected by tides along the shelf edge over much of the Great Barrier Reef (Fig. 1). In total, tidal currents are estimated to dominate sediment transport on about 17.4% of the Australian shelf (Fig. 1; Harris, 1995).

Generally, tidally dominated shelves display discrete zones of seabed scouring and erosion coinciding with regions of the shelf subject to maximum tidal bed stress (Harris et al., 1995). An important distinction from storm dominated shelves is that the facies on tidally dominated shelves have boundaries that are aligned more or less at right angles to the coast (Walker, 1984). Sediment facies are arranged in a divergent pattern that reflects an increasing supply of sand of decreasing grain size with increasing distance away from the scour zone (Harris et al., 1995). Such diverging bedload transport patterns are known as bedload partings (Johnson et al., 1982). Regions of the Australian continental shelf where tidal currents have produced strong bedload parting facies include the Torres Strait, the Gulf of Carpentaria (Harris, 1994) and Whitsunday Islands (Heap, 2000). In these regions, tidal currents are accelerated as they flow through constricted channels located between islands and reefs. The zones of maximum tidal current speed are sometimes related to tidal amphidromic points. These are a type of standing wave node in which sea level change is small but current speeds are large; two such amphidromic points are found in the Gulf of Carpentaria (Harris, 1994).

1.3. Shelves dominated by intruding ocean currents

Intrusive ocean currents that cause sediment transport (Fig. 1) affect less than 1% of the Australian shelf. These currents are dominant offshore from Fraser Island, where the southward flowing East Australian Current intrudes onto the shelf and a coarse-grained rhodolith gravel pavement has been deposited (Harris et al., 1996). Sidescan sonar and seabed photographs, obtained during the 1980 cruise of the German research vessel *Sonne* to the northern NSW and southern Queensland region, reveal large subaqueous dunes at water depths as great as 80 m (Jones and Kudras, 1982). Dune morphologies indicate a general southward transport of sand, which Gordon and Hoffman (1986) attributed to the East Australia Current. The Leeuwin Current has a similar effect over parts of the Western Australia shelf (Pearce and Pattiaratchi, 1997).

2. Methods

2.1. Threshold exceedance due to swell waves

Using Airy, first-order wave theory (Komar and Miller, 1973), we have estimated the wave-induced threshold of sediment for observed grain size distribution around the continental shelf. Currents produced by the passage of a shallow water wave are reduced to backward and forward motions, having an orbital diameter d_o. Over the wave period T, the velocity at a fixed point on the bed will vary from zero to a maximum U_{max} according to the relationship.

$$U_{max} = \pi d_o / T = \pi H / [T \sinh(2\pi h/\lambda)] \quad (1)$$

where H is the wave height (m), h is the water depth (m) and λ is the wavelength of the surface gravity wave (m) (Komar and Miller, 1973). When the near-bed current accelerates from zero towards a maximum value (U_{max}), it may exceed the threshold value (U_{cr}) where a specific sediment grain size is mobilised. Although more accurate estimates of U_{max} are possible by using a spectral wave current model (Madsen, 1994), the necessary wave data are not available. Estimates of U_{max} derived from Eq. (1) give an accurate result away from the shoreface zone in water depth greater than 5 m and under the near-threshold and deep water shelf conditions that are of interest in the present study (Hardisty, 1994).

2.1.1. Australian wave model

In this study, surface wind speed estimates generated by the Australian Bureau of Meteorology's regional atmospheric model provided input to the Wave Model, WAM (Hasselman et al., 1988; Komen et al., 1994) to yield estimates of mean wave height and period. The data are six-hourly predictions of significant wave height (SWH), period and mean wave direction, gridded at 0.1° spatial resolution, for the period March 1997 to February 2000, inclusive. The WAM model is run operationally at many forecasting centres around the world, including a version at the Australian Bureau of Meteorology. When compared to observations of SWH from wave-rider buoys around the Australian coast, the rms error of forecast SWH is approximately 0.5 m. The source terms and propagation terms are integrated every 5 min. In terms of the wave spectrum, the directional resolution is 15° and there are 25 frequency bins ranging from 0.0418 to 0.4114 Hz. This represents wave periods from approximately 24–2.5 s.

This high-resolution wave model (0.1°) was nested within a regional wave model (1°), which spans the oceans around Australia, ranging from latitudes 60°S to 12°N and longitudes 69°E to 180°E. The spectral resolution was the same for both models. The regional wave model (1°) provided the boundary conditions for input to the high-resolution wave model (0.1°). This regional wave model, in turn, was nested within a global model (3°).

Although we are concerned here with the impact of the water waves on the bed sediment, the seafloor in turn affects the form and propagation of surface waves. The major impact on the modelled wave height due to the water depth is that when $h<\lambda/4$, an extra source term must be included in the wave models, representing the dissipation of wave energy due to bottom friction. Other shallow water effects, such as depth-induced breaking are not included in WAM, and for this reason, a water depth of approximately 20 m is considered to be the shallowest depth to which it is possible to run WAM successfully (Booij et al., 1999).

In Eq. (1), water depth (h) was approximated from Geoscience Australia's (formally the Australian Geological Survey Organisation (AGSO)) bathymetry database. This bathymetric model was interpolated to a grid spacing of 0.01°. The high-resolution wave model outputs were then combined with the bathymetry grid, and Eqs. (1)–(3) were solved at six-hourly intervals. The number of times that the threshold value was exceeded at each bathymetric grid point was then summed to produce threshold exceedance maps of Australia's continental shelf region for observed grain size.

To quantify the synergy of wave height and period around Australia, wave power P was calculated as follows:

$$P = pg^2H^2T/32\pi \tag{2}$$

2.1.2. Estimation of wave threshold exceedance

The threshold speed (U_{cr}) is a function of the wave period, boundary layer thickness, bed roughness, grain density and shape, water viscosity and whether or not the grains are cohesive or cemented (e.g. Grant and Madsen, 1979, 1986; Hammond and Collins, 1979; see review of Hardisty, 1994). Simplified empirical threshold equations have been published by Clifton and Dingler (1984), for flat-bed, spherical, cohesionless, quartz silt and fine sand. For silt and fine sand and grain size $D<0.05$ cm in diameter the threshold speed is given by:

$$U_{cr} = 33.3(TD)^{0.33} \tag{3}$$

and for coarse sand and gravel (D>0.05 cm):

$$U_{cr} = 71.4(TD^3)^{0.143} \tag{4}$$

Although the viscosity of water varies with temperature and salinity, these are held constant in Eqs. (3) and (4) (Clifton and Dingler, 1984).

2.1.3. Sediment grain size distribution on Australian continental shelf

The observed mean grain size of sediment on the Australian continental shelf was provided from the sediments database auSEABED (Jenkins, 2000; Fig. 3). The grid representing sediment grain size for the shelf was generated from the September 2000 data content. In total there were in excess of 180,000 sites made up of both descriptive and quality controlled analyses. The descriptive data from known sites were parsed and used along with the analyses to glean as much information as possible about the distribution of sediment grain sizes on the shelf. The statistical confidence of these descriptions is documented in Jenkins (2000). To convert these data from auSEABED into a grid, the data representing mean grain size were converted from phi to millimetres and linearly interpolated to give a continuous surface. It is acknowledged that some areas of the shelf are not as reliable as others due to the spatial distribution of sample sites. This is particularly true in the Gulf of Carpentaria and parts of the North West shelf.

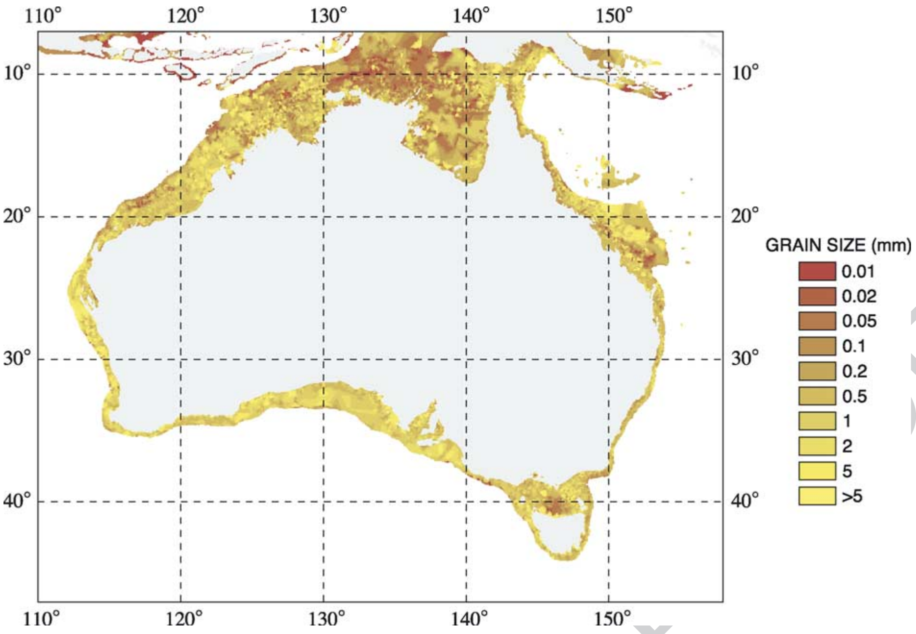

Fig. 3. Mean grain size of sediments on the Australian continental shelf derived from the AUSEABED database (Jenkins, 2000).

2.2. Threshold exceedance due to tidal currents

Threshold exceedance was estimated for unidirectional, steady flow conditions using the empirical curves of Miller et al. (1977). This graph is based on the results of selected open-channel, straight-sided flume experiments conducted by various investigators, using standard laboratory conditions (i.e. an initial flat bed, cohesionless quartz spheres under steady, fresh water flows at 20 °C). The data specify an empirical formula which gives threshold exceedance for quartz spheres less than or equal to 2 mm under the above described laboratory conditions, as:

$$U_{100} = 122.6D^{0.29} \quad (5)$$

where U_{100} is the threshold current speed referenced to 1 m above the seabed and D is the grain diameter in mm. Hourly averaged, tidal current speeds were estimated using a hydrodynamic tidal model for the Australian shelf, derived specifically to meet the spatial–temporal requirements of the present study.

2.2.1. Australian tide model

An ocean tide model for the Australian shelf was set up for the region limited by 0°S to 45°S and 109°E to 160°E (Harris et al., 2000). The resolution of the model is 0.067° in both latitude and longitude. This corresponds to 7.4 km at the equator and 5.2 km at the southern-most latitude of the model domain. In the longitude direction, it corresponds to 7.4 km.

The linearized, shallow-water, tide model described by Egbert et al. (1994) was used. Dissipation was approximated using a quadratic expression with depth (h)

$$K = K_0/(\max(h, h_0)^2 \quad (6)$$

where K_0 is the bottom drag coefficient at depth h_0. At shallower depth, dissipation is equal to K_0. A parameter choice of $K_0 = 0.05$ and the minimum depth of $h_0 = 20$ m was made after extensive testing as it worked well for most regions. In the Bass Strait, the model produced too small amplitudes, which was subsequently compensated for by the data assimilation (see below).

Geoscience Australia's bathymetry on a 1-min (1.8-km) grid was used and re-interpolated onto the 15 min resolution grid used for the model. However, this database suffers from frequent loss of coverage for several regions in the deep ocean. In these regions it was supplemented with data obtained from the

National Geophysical Data Center (NGDC) bathymetry model (Smith and Sandwell, 1997)

The model includes the major eight constituents M_2, S_2, N_2, K_2, K_1, O_1, Q_1, P_1. The solution was obtained using time stepping on an Arakawa C grid by applying periodic forcing and time stepping from homogenous initial conditions. The solution was achieved in 10,000 time steps using a step length of 15 s. This corresponds to running the model for roughly 2 days. Along the open boundaries around the edges of the model a global ocean tide model by Andersen et al. (1995; version AG95.1) was used to provide boundary elevations (see also; Shum et al., 1997).

2.2.2. Assimilated altimetry and tide gauge data

Satellite observations of sea surface height were initially used to derive harmonic constituents at the location of observations. The altimetric observations were derived from the NASA ocean altimeter Pathfinder products for the TOPEX/POSEIDON satellite. A full description of the data sets, their editing and processing can be found at http://www.neptune.gsfc.nasa.gov/ocean.html. A total of 179 crossover solutions obtained from TOPEX/POSEIDON altimetry were located inside the domain of the model.

The Australian National Tidal Facility provided a set of harmonic constituents for 57 primary ports in Australia. Harmonic constituents from 16 of these ports were used to supplement the altimetry, resulting in a total of 195 tidal constituent sets, which were "blended" into the hydrodynamic tide model as described below. Harmonic constituents from the remaining 41 ports were used to tune and validate the tidal model.

Altimetry and tide gauge data at these 195 locations within the model domain were incorporated into the hydrodynamic model using a simple assimilation procedure called blending. The technique is similar to the method introduced to tidal modelling by Kantha (1995) for a global case.

In this procedure, the predicted tidal height at the 195 locations is substituted by a weighted mean of the predicted tidal height (H_{pred}) by the model and the observed height (H_{obs}) by the satellite or tide gauge, as:

$$Ht = wH_{\mathrm{obs}} + (1 - w)H_{\mathrm{pred}} \tag{7}$$

where the prediction weight w is determined for each constituent individually. The modified height Ht is subsequently used to calculate the velocities for the subsequent timestep.

The weights for the blending were determined upon testing that the model is kept spatially smooth around the location of the blending. For diurnal constituents obtained from altimetry, $w = 0.85$ and for diurnal constituents $w = 0.75$. For harmonic constituents derived at tide gauge ports a weight of 0.97 was used. The blending was only performed at each 10th timestep because of the way that the asymptotic model is sampled to obtain the harmonic constituents.

2.2.3. Estimation of tidal current threshold exceedance

The problem of calculating the bottom stress using modelled current speeds is that the effect of the benthic boundary layer is difficult to model in deep water (e.g. Pingree and Griffiths, 1979). The tidal model used here generated depth-averaged, hourly averaged currents, and ignores the effects of bottom roughness elements and other bathymetric features affecting the velocity profile.

The Australian shelf model was subsequently time-stepped through a spring-neap cycle (roughly 2 weeks) at hourly intervals. The tidal current speeds were bi-linearly interpolated to a grid spacing of 0.01° to conform to the swell wave exceedance calculations. Based on the threshold curve for unidirectional currents published by Miller et al. (1977; Eq. (5)) occurrences of threshold exceedance were tallied for the hourly current speed at each grid point to then generate a percentage of threshold exceedance map of the Australian continental shelf. As with the wave model the observed grain size data for the Australian continental shelf was provided from the sediments database auSEABED (Jenkins, 2000).

2.3. Relative significance of wave versus tidal current threshold exceedance

Waves or tides (or both) may affect sediment mobilisation on continental shelves, but the question posed here is which process dominates over the other on the Australian continental shelf? For the purpose of our analysis, threshold exceedance by waves occurring during any 6-h period is registered as an "event".

The number of events per year yields a percentage of time for wave threshold exceedance for a given grid point.

For tides, threshold exceedance by the hourly averaged bottom stress over a spring-neap cycle implies that movement occurs at least every fortnight (or 26 times per year). Thus, the main difference between wave and tidally effected shelf areas is that, whereas tidal exceedance is periodic (fortnightly), the wave exceedance is episodic and/or seasonal. The sources of error in the analysis are thus also different for each case.

Below we assess the relative importance of waves and tides in mobilising the unconsolidated seabed sediments on the Australian continental shelf by accounting for the percentage of time that each process exceeds the threshold for mobilising the observed mean grain size. The analysis is carried out for each modelled grid point and the data are used to generate maps showing the spatial distribution of wave- and tide-dominated threshold exceedance.

3. Results

3.1. Waves

Around Australia, annual mean wave power is greater in the southern waters than in the northern waters (Fig. 4). The largest and longest-period (most powerful) waves occur off the west coast of Western Australia, in the Great Australian Bight and off western Tasmania (Fig. 5). Low mean heights and shorter periods occur on the Northwest Shelf, the Arafura Sea and in the Gulf of Carpentaria (Fig. 4). This pattern of wave climate is generally consistent with previous studies of waves on the continental shelf around Australia (e.g. Louis and Radok, 1975; McMillan, 1982; Wolanski, 1985).

Maximum wave power peaks at 2 mW per m^2 in the southern Great Barrier Reef, close to the Marion Plateau (Fig. 5), associated with waves generated by Tropical cyclone conditions. Wave power attained 0.76 kW per m^2 in the central Gulf of Carpentaria associated with cyclone Sid, which is nearly 200 times the mean wave power at this location (Figs. 4 and 5).

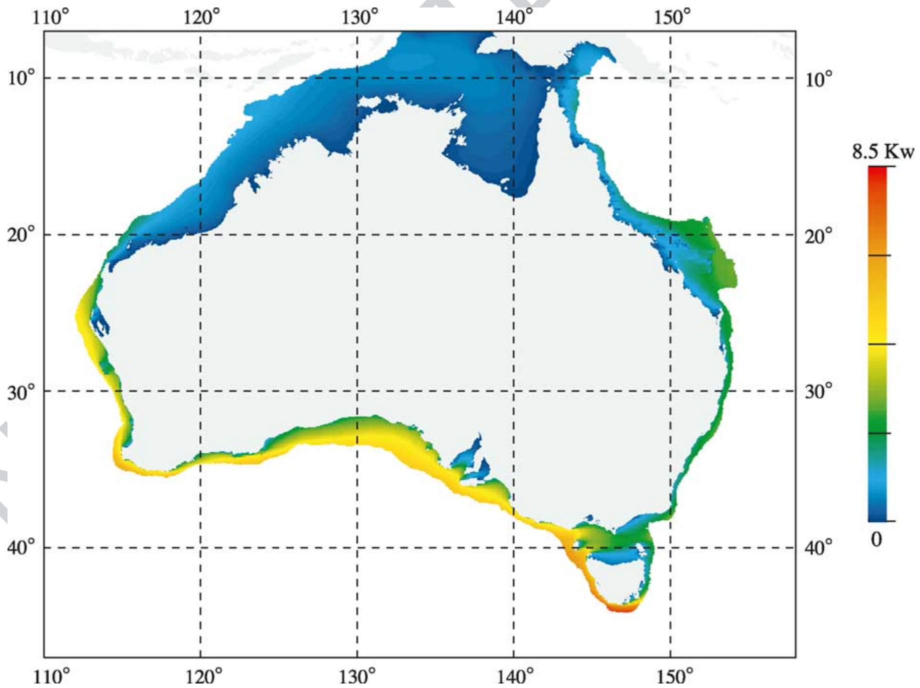

Fig. 4. Mean annual wave power (W/m^2) for the period March 1997 to February 2000, inclusive.

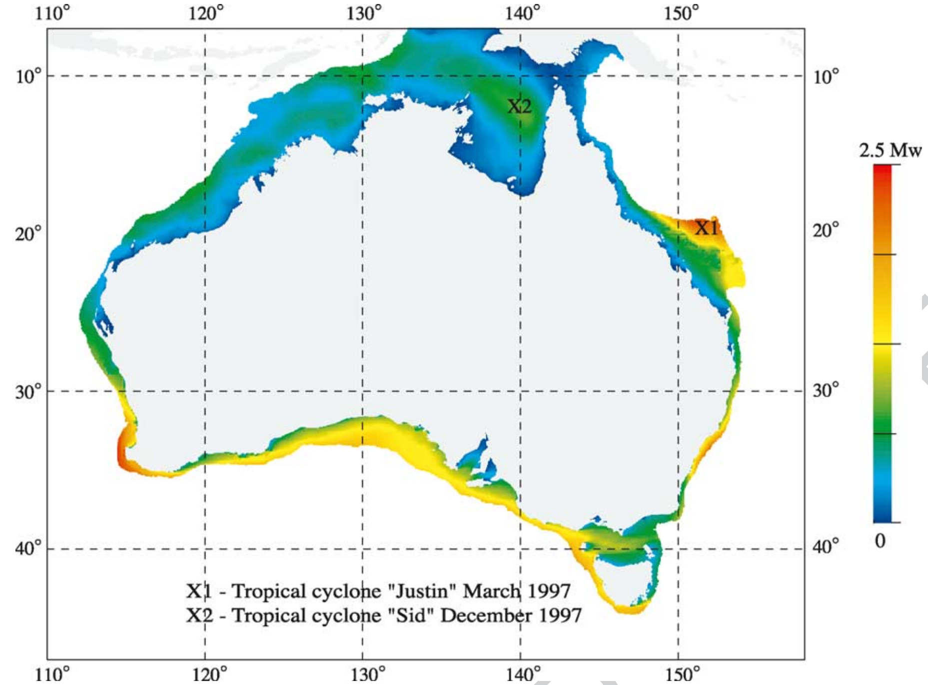

Fig. 5. Maximum wave power (W/m^2) for the period March 1997 to February 2000, inclusive.

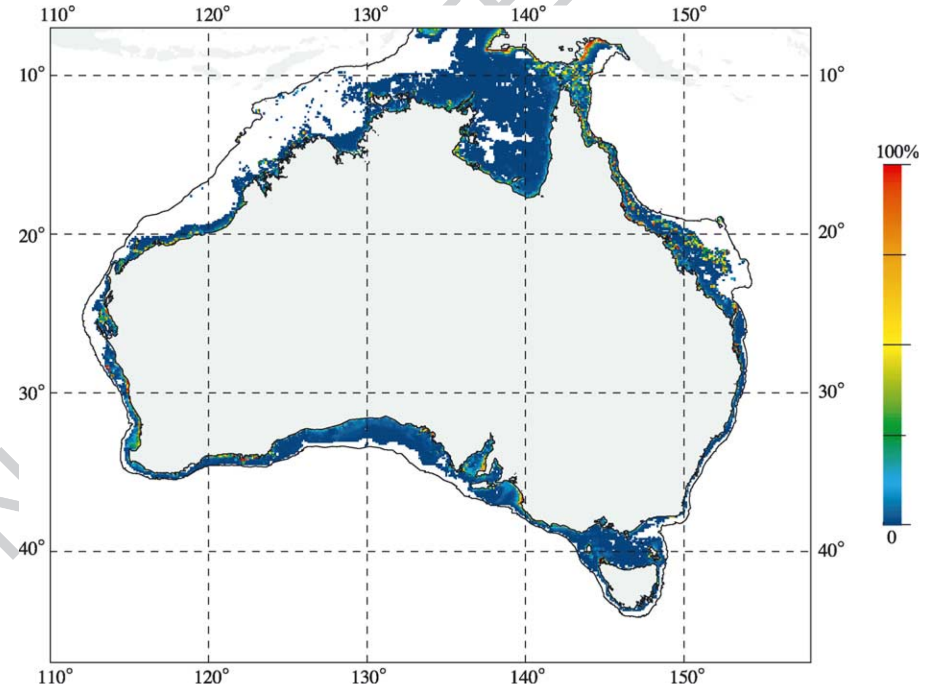

Fig. 6. Wave induced exceedance for observed grain size distribution on Australian continental shelf for the period March 1997 to February 2000, inclusive.

A feature of our prediction (Figs. 4 and 5) is the occurrence of quiet zones on the lee sides of islands and within protected embayments including King and Flinders Islands in Bass Strait (Fig. 4) which are protected from the prevalent weather. However, diffraction and refraction are not accounted for in the wave model used here, and so these protected zones are probably overestimated to a certain extent.

3.2. Threshold exceedance due to swell waves

The results indicate that threshold for mean grain size was exceeded over ~31% of the shelf by waves between 1997 and 2000. The coarsest sediment appears to be in the temperate regions (Fig. 3). There is generally a landward succession of zones of increasing threshold exceedance, which is particularly clear on broad shelves such as the Great Barrier Reef, Gulf of Carpentaria, Lacepede Shelf and the Gulf of Papua (Figs. 2 and 6).

The precise locations where the most powerful waves in the oceans around Australia are found varies from year to year, depending on the frequency/duration of storms and prolonged high wind speeds over a large fetch (e.g. Vincent, 1986; Harris and Coleman, 1998). The maximum wave height and period occurring on the shelf translates into a maximum water depth of potential shelf sediment mobilisation (depending on grain size). During the 3 years of modelled wave power, the maximum occurred in the southwest off Cape Leeuwin and eastern Marion Plateau. The deepest sediment mobilised was 0.005 mm on the Marion Plateau at a depth of greater than 300 m.

3.3. Tides

Generally, the strongest tidal currents occur on macrotidal shelf areas (Fig. 7). Along the northwestern coastline of Australia, a maximum spring tidal range of 12.5 m is reached in Collier Bay, King Sound (Fig. 2; Easton, 1970). On the shelf adjacent to King Sound, our modelling results show maximum tidal current speeds ranging up to around 1.5 m/s. For eastern Queensland, our modelling results show the shelf is characterised by relatively high maximum tidal currents in the Torres Strait and Broad Sound

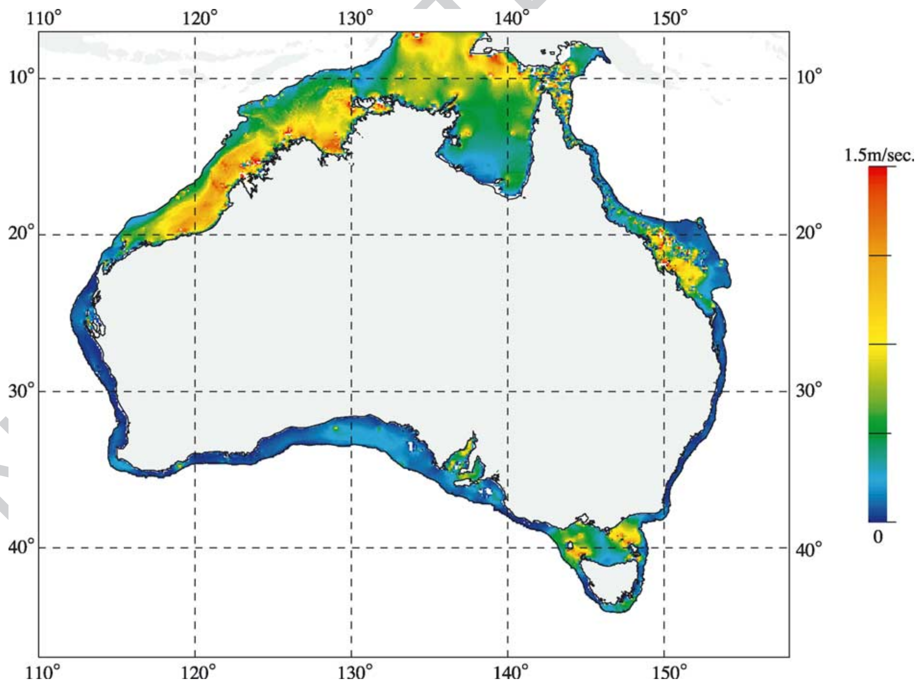

Fig. 7. Mean spring tidal current speed on the Australian continental shelf.

areas (Fig. 2) which has a tidal range of up to 8.2 m (Cook and Mayo, 1978).

Tidal currents are also relatively strong in some mesotidal and microtidal gulfs and shelf seaways, such as the Gulf of Carpentaria, Spencer Gulf, Gulf of St. Vincent, Bass Strait and Torres Strait. Amphidromic points located in the Gulf of Carpentaria, Joseph Bonaparte Gulf and in Bass Strait (Harris, 1994) are locations of tidal current maxima (Fig. 7).

3.4. Threshold exceedance due to tides

Tidal currents exceed the threshold speed for the mean grain size over ~41% of the shelf. The spatial distribution of tidal threshold exceedance (Fig. 8) illustrates that tidal currents are competent to mobilise finer sediments in the silt to fine sand range over most of the northern and northeastern sections of the shelf, including Bass Strait, Shark Bay and in Spencer Gulf. In contrast, gravel is locally mobilised mainly on the inner shelf at the sites of strongest tidal flows such as Torres Strait. In macrotidal King Sound, sand of up to 0.35 mm in diameter is mobilised 100% of the time.

4. Discussion

4.1. Derivation of a new shelf regionalisation

Combining the wave and tidal exceedance estimates into a ratio allows an assessment of the relative spatial importance of these two mechanisms in mobilising bottom shelf sediments (observed mean grain size, Fig. 3). Based on this approach, we have defined six separate categories of continental shelf region. Shelf regions where neither wave nor tidal currents were capable of mobilising bottom sediment are classified as "zero-mobility" regions. Shelf regions where either waves or tides mobilised the bottom sediment are classified as "wave only" or "tide only". Shelf regions where both waves and tides are capable of mobilising sediment are classified as "wave-dominated", "tide-dominated", or "mixed" depending upon the relative amount of time that each process is competent in mobilising the bed sediment. Our definition of "wave-dominated" applies to locations where the percentage of time of wave mobilisation is greater than three times the percentage of time

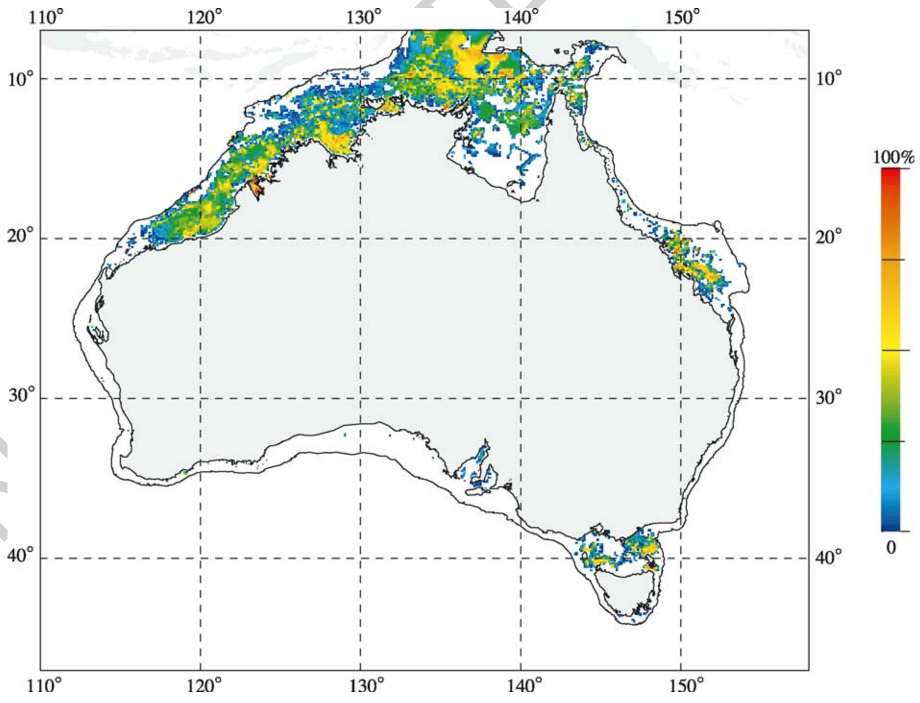

Fig. 8. Tidal induced exceedance for observed grain size distribution on Australian continental shelf.

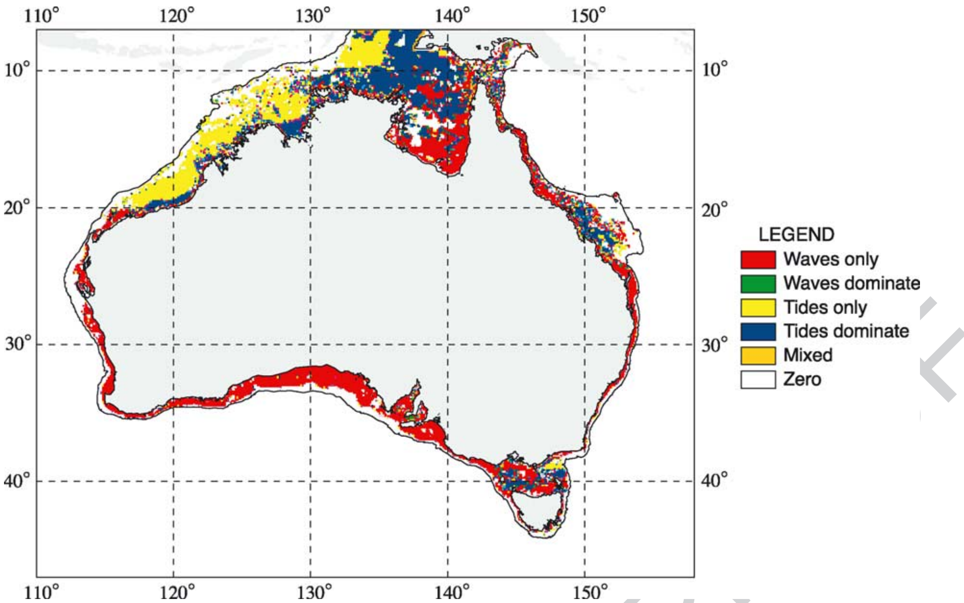

Fig. 9. Regionalisation of the Australian continental shelf for observed grain size distribution based on ratio of wave and tidal exceedance estimates.

of tide mobilisation. "Tide-dominated" applies to locations where the percentage of time of tidal mobilisation is greater than three times the percentage of time of wave mobilisation. Finally, "mixed" regions are defined here as occurring where the ratio of wave/tidal percent time exceedance is between 1/3 and 3. This concept of mixed wave and tidal current energy in mobilising bottom sediments is well established in the literature (e.g. Grant and Madsen, 1979, 1986; Pattiaratchi and Collins, 1985; Lyne et al., 1990).

The spatial distribution of our six regions (Fig. 9) indicates that they are not equal in surface area (see Table 1). However, increasing or decreasing the ratio of "3" only results in the increase of some regions at the expense of others. For example, wave-dominated and mixed areas are both small (~ 0.5% and ~ 2% of the shelf, respectively; Table 1) and the area of one of these regions can only be increased at the expense of the other. The spatial extent of the wave-only region (~ 30% of the shelf) and the tide-only region (~ 22% of the shelf; Table 1) are mutually exclusive and their surface area is not affected by the definition of wave-dominated, tide-dominated or mixed regions.

Table 1

km^2	% SHELF	Mean depth (m)	Mean carbonate content (mm)	Mean grain size (mm)	Mean mud content (%)	Mean sorting
768,508	30.22	48.55	72.66	0.88	13.32	1.36
12,345	0.49	22.63	63.79	0.39	26.86	1.72
571,559	22.47	47.98	72.69	0.29	40.96	2.16
466,144	18.33	111.32	76.93	0.57	24.21	1.61
48,403	1.90	24.85	70.56	0.43	25.53	1.66
676,199	26.59	188.78	83.65	1.95	14.67	1.52

Overall, there is a good spatial correspondence between our modelling results (Fig. 9) and the intuitive shelf classification proposed by Harris (1995; Fig. 1), although there are some disparities. For example, our results show Spencer Gulf, is "wave-dominated" and mixed (Fig. 9), whereas Harris (1995) predicted that this region was dominated by tidal currents (Fig. 1).

4.2. Regions of zero sediment mobilisation

Although we have focussed on near-bed currents generated by tidal and swell-wave processes, shelf currents occur at a number of different spatial and temporal scales: at the scale of turbulence (0.2–5 s); at the scale of wave orbital currents (5–20 s); at the scale of tidal currents (6 h); and at the scale of storm events

(6–10 days). Superimposed upon these "events" will be other currents, such as intruding ocean currents, which may flow at a steady rate for weeks or months without changing significantly in speed or direction. The current regime in any given area is the product of a combination of different current components, although one type may be dominant locally (e.g. Swift et al., 1971). There are also areas of the shelf where the total energy available to mobilise the bottom sediment is very low.

Our results indicate that the region of zero mobility accounts for ~27% of the shelf. Combined wave and tidal currents are capable of mobilising and transporting quartz grains of a given size in deeper water and in shallow water more frequently. Furthermore, in shallow areas with a large tidal range, swell waves are most effective at mobilising sediment towards low water (i.e. when the water depth is at a tidal minimum). Under these circumstances, sea level variations must also be taken into account in the estimation of sediment mobilisation under combined flows. However, our interest is in the relative importance of waves and tides (i.e. determining areas of tide- versus wave-dominated transport) rather than the absolute value of transport intensity under combined flow conditions.

Although oceanographic processes other than waves and tides may influence sediment mobilisation, to a first approximation the zero-mobility regions defined here may be expected to behave as low-energy, depositional environments. In the present study, sediments deposited in zero-mobility regions occur at the greatest mean water depth (mean of 189 m) and are found to be more coarse-grained (mean size of 1.95 mm), higher in carbonate content (83.7%) and relatively lower in mud content (14.7%) in comparison to other shelf regions (Table 1). This finding contradicts the concept of a graded shelf (Swift and Thorne, 1991) and Aigner's (1985) "proximality" diagram, in which mud content and the rate of bioturbation increase in an offshore direction (with lower energy and increasing depth). The explanation is that widespread occurrence of coarse, carbonate sediments on outer portions of the Australian continental shelf has been attributed in many areas to their relict origin (e.g. Jones, 1973; Davies, 1979; Jones and Davies, 1983). These relict deposits appear generally not have been buried by fine-grained, muddy sediments, probably because of the small volume of sediment discharge by Australian rivers, much of which is trapped within coastal depositional environments (Harris et al., 2002).

We conclude that Australia's deep-water, outer-shelf sediments are not in equilibrium with modern tide and wave hydrodynamic processes. Previous researchers have shown that in at least a few locations (i.e. off Fraser Island and sections of the east Australian margin) the deposition of coarse-grained carbonates is affected by strong ocean boundary currents. The question remains as to how much of the zero-mobility region is influenced by such ocean currents. Further field-research and modelling studies are required to find the answer to this question.

4.3. Mean grain size in relation to wave-only and tide-only mobilisation regions

The results of our analysis allow comparisons to be made between the areas of the Australian continental shelf where sediment mobilisation is affected by swell waves or tidal currents, and the associated water depth, carbonate content and grain size distribution (Table 1). The association between regions of zero-mobility and water depth, carbonate content and grain size distribution were described above.

The wave-only and tide-only regions have nearly identical mean water depths (23 to 25 m) and mean carbonate contents (both 73%) but very different mean grain size properties. Sediments in wave-only regions are coarser, lower in mud content and better sorted than sediments in tide-only regions (Table 1). Further insight is provided by a plot of mean grain size versus wave power and tidal current speed (Fig. 10). These plots show that, whereas there is a weak relationship between increasing tidal current speed and increased grain size ($R = 0.38$; Fig. 10A), there is no evident correlation between mean grain size and increasing wave power (Fig. 10B). Apparently, wave-only regions are more efficient at winnowing and dispersing mud and finer-grained sediment, leaving a coarse, sorted lag deposit. In contrast, some tide-only regions appear to trap fine sediment particles, as supported by previous observations of tidal turbidity maxima at several locations around Australia, including Gulf St. Vincent (Phillips and Scholtz, 1982), King Sound (Semeniuk, 1982) and Torres Strait (Harris and Baker, 1991). The results of our analysis of tidal currents

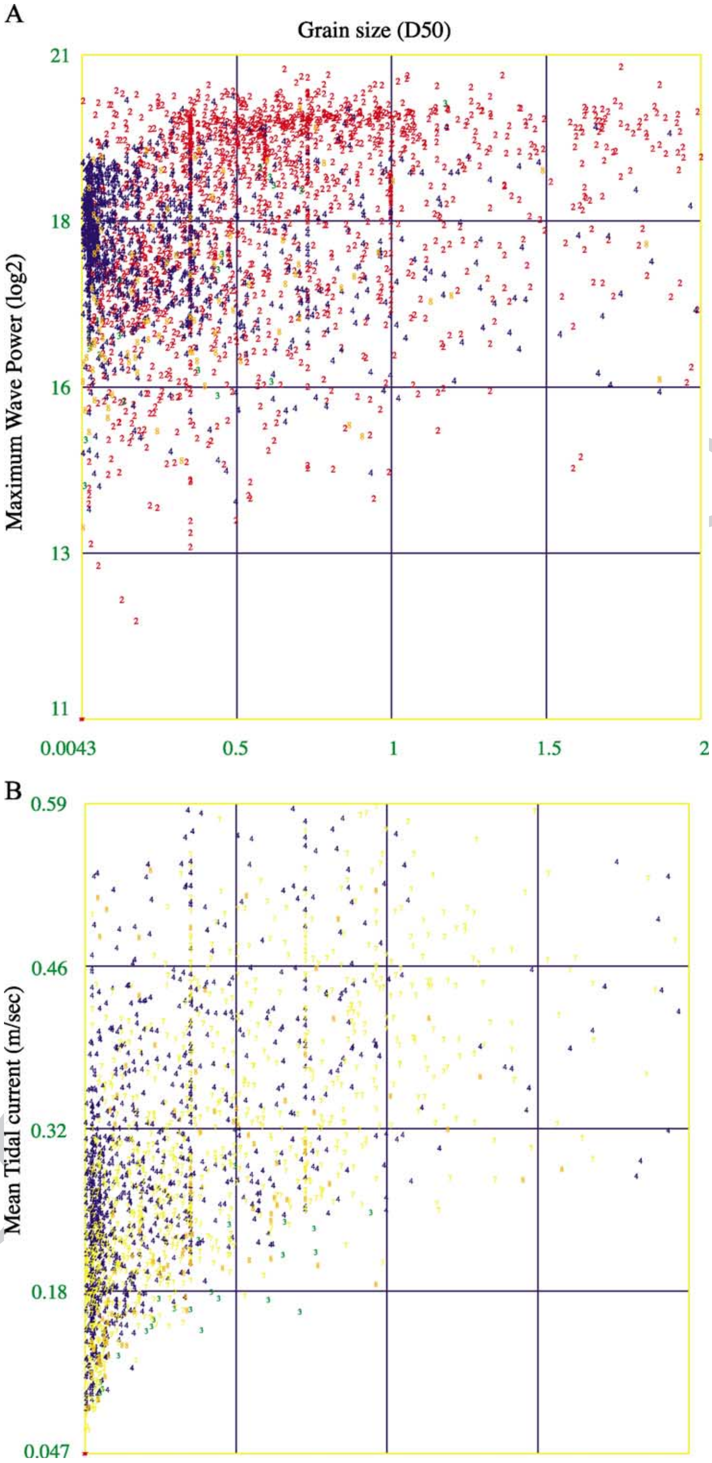

Fig. 10. Scatter plots of mean grain size versus: (A) $\log_2$ of maximum wave power (W/m^2) for the period March 1997 to February 2000, inclusive; and (B) mean tidal current speed (m/s).

and bottom sediments in tide-only regions, indicates that areas of the North West Shelf and Bonaparte Gulf (Fig. 1) having bottom sediments with high mud-content are associated with peak tidal current vectors directed landwards and along the coastline (Fig. 11). In contrast, areas of low mud content are associated with seaward directed maximum tidal current vectors. In regions where tidal processes control sediment transport, mud appears to be trapped on flood-dominated shelves but not on ebb-dominated shelves.

Calcareous detrital silt is also generated in tidal shelf environments by the disintegration of soft carbonate grains as they are transported during bedload transport (Harris, 1994), which explains the high mud content (41%) of tide-only regions (Table 1). This high mud content is potentially of interest to environmental managers because heavy metals are commonly absorbed onto the surfaces of fine-grained sediments (e.g. Bourg, 1987). For example, the highest concentrations of heavy metals are found in the muddy deposits of Spencer Gulf (Harbison, 1984) and Torres Strait (Baker and Harris, 1991).

Tropical regions of Australia are prone to rare cyclone storm events. The sections of the shelf most frequently affected by cyclones are the North West Shelf with an average of 10 cyclones per decade, the Gulf of Carpentaria 6 cyclones per decade and the Great Barrier Reef 4–5 cyclones per decade (Fig. 1). Tropical storms are episodic and infrequent (Fig. 1) with the time between events being measured in years. Between these violent storm events, amounts of fine sediment are likely to accumulate and are only mobilised when another event occurs.

In contrast with the tropics, temperate regions experience frequent low-pressure systems and related

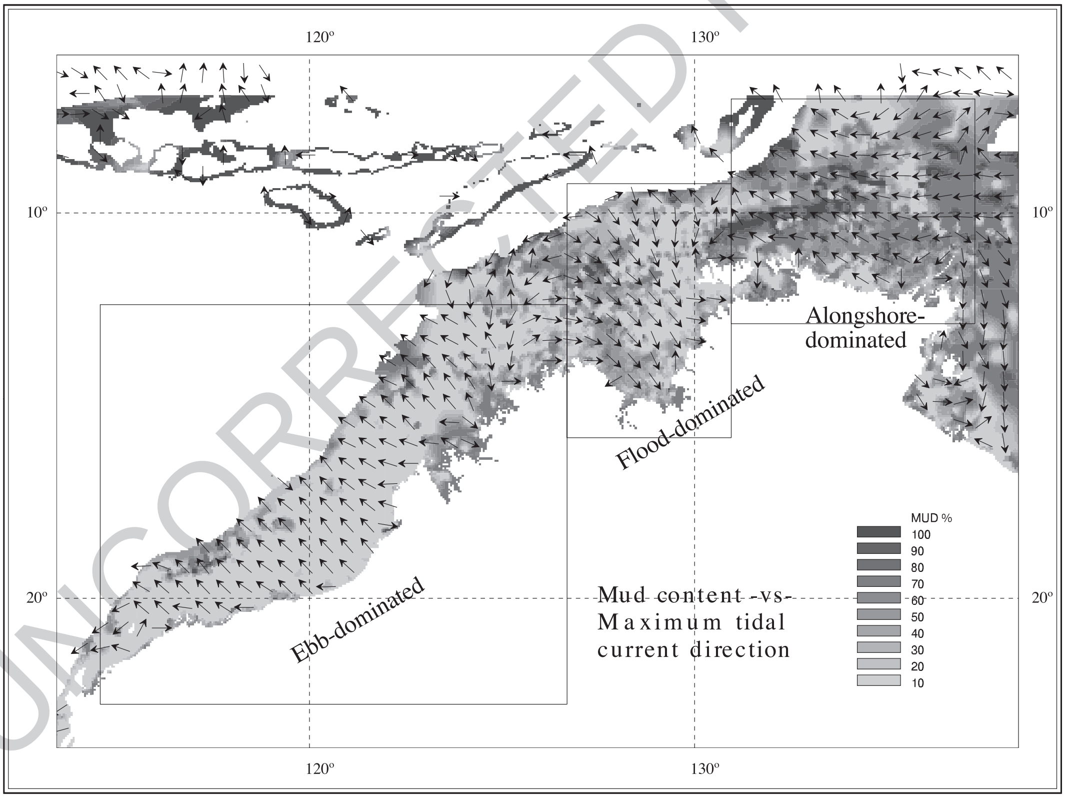

Fig. 11. Map of the northern Australia continental shelf, showing the mud content of surficial sediments in relation to the direction of maximum tidal current vectors. Muddy sediments appear to be associated with landward and along-shelf vectors, whereas low mud content is associated with off-shelf oriented vectors.

storm events (Fig. 12). Large swell waves in temperate regions (Fig. 4) are the result of a continual series of cold fronts passing eastwards across the Southern Ocean. They are responsible for gale force winds producing large amplitude, long-period swell waves in places like southwest Australia and Bass Strait (Fig. 4). The propagation direction of storms in this region is usually towards the east. For example, the profile of a large storm in southwest Australia during October 1997 can be seen a few days later in Bass Strait (Fig. 12).

Currents produced by swell waves winnow away fine sediments, leaving a sorted layer of coarser sediment, which armours the seabed against further mobilisation. The equilibrium is only broken when a storm is violent enough to remove the armoured layer to allow

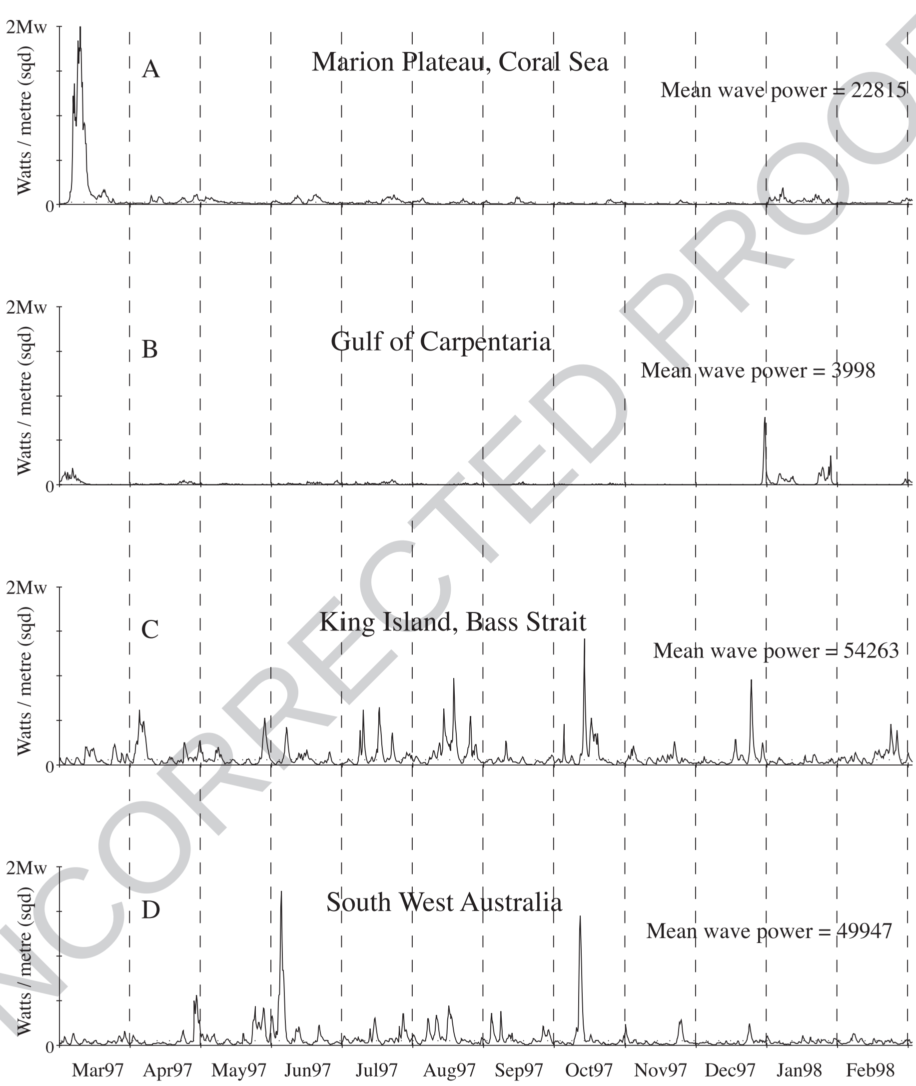

Fig. 12. A time series of wave power for four locations (shown in Fig. 2) (A) Marion Plateau; (B) Gulf of Carpentaria; (C) Bass Strait; and (D) Rottnest Shelf, southwest Australia. The 18 kW per m^2 wave power peak on the Marion Plateau occurs in March 1997 at the same time tropical cyclone Justin was active over the Coral Sea and Queensland coast (X1 in Fig. 5). Wave power attained 10 kW per m^2 in the central Gulf of Carpentaria in December 1997, coincidental with Tropical cyclone Sid. (X2 in Fig. 5). This result is >20 times the mean wave power at this location.

the winnowing process to start again. For this reason, wave-only regions of the Australian shelf (Fig. 9) are associated with the coarsest-size sediments (0.88 mm; Table 1) and coarser sediments generally coincide with the largest maximum wave power (Fig. 10).

4.4. Sediment mobility and benthic biological habitats

Sedimentologists generally focus on the preserved fossil assemblage and rarely consider the entire suite of living organisms that may be associated with a given core site or sedimentary environment. Biologists are equally biased in their research, as much more has been published on ecosystems associated with hard substrates (e.g. rocky shores and coral reefs) than ecosystems associated with unconsolidated sediment (Gray, 1981). Studies by Somers (1987), Long et al. (1995) and Kostlyev et al. (2000) have illustrated the link between the texture and composition of bottom sediment with the distribution and abundance of benthic species. Shepherd (1983) and Poiner and Kennedy (1984) showed that the biodiversity and abundance of benthic species is inversely related to the mobility of the substrate, with the lowest abundance and diversity associated with bedforms. From this perspective, the high energy, mixed and tide-dominated zones of eastern and western Bass Strait comprise coarse-grained carbonate dunes (also termed "sandwaves"), which coincide spatially with a large part of scallop trawl-grounds (Kailola et al., 1993). It follows, therefore, that on sediment-mantled continental shelves, benthic habitats can be distinguished by sediment composition and grain size properties, together with the rate of sediment transport, and the frequency of the resuspension of detritus during storm and current events (Todd et al., 2000). On such continental shelves, measurements of sediment mobility can provide the basis for predicting the spatial and temporal nature of benthic habitats.

5. Conclusions

Using estimates of tidal current speed and significant wave height and period we have generated a new regionalisation of the Australian continental shelf, differentiating between wave- and tide-dominated shelf environments. The relative distribution of these regions is not dissimilar from the conceptually based regionalisation proposed by Harris (1995).

Our models, applied to the observed mean grain sizes, predict that sediments are mobilised by waves on ~31% of the continental shelf and by tidal currents on ~41% of the shelf. Thus, mobilisation of sediment on the Australian continental shelf is due mostly to tides rather than waves, in contrast to earlier models. Although the wave-only and tide-only regions of sediment mobilisation are found in similar water depths (mean depth of around 48 m) and the sediments have comparable carbonate content (mean of about 73%) the grain distributions are quite dissimilar. Tide-only regions have a mean grain size of 0.29 mm, and a mean mud content of 41%, compared with 0.88 mm and 13%, respectively, for wave-only mobilisation regions. We attribute these grain size patterns to differential winnowing and trapping of fine sediments by wave and tidal processes, and in particular, to the more efficient generation of calcareous silt by the fracturing of soft carbonate particles in tide-only regions. Trapping of mud on the shelf is associated with landward and along-shelf oriented maximum tidal current vectors, whereas off-shelf directed current vectors are associated with low mud content deposits.

The zero mobility region, located in deep water (189 m mean depth), is characterised by coarse-grained, calcareous sediments having a low mud content. This contradicts the conventional, graded shelf model but is consistent with earlier reports of widespread relict sediment deposits on the outer shelf and upper slope. These coarse-grained, relict carbonates are not in hydraulic equilibrium with the prevailing tide and wave current regime, but are known to be influenced in some locations by strong ocean boundary currents. Further research is needed to establish the spatial extent of ocean current influence on sediment mobilisation over Australia's continental shelf.

References

Aigner, T., 1985. Storm depositional systems. Lecture Notes in Earth Sciences, vol. 3. Springer-Verlag, Berlin. 174 pp.

Andersen, O.B., Woodworth, P.L., Flather, R.A., 1995. Intercomparison of recent global ocean tide models. J. Geophys. Res. 100 (C12), 25261–25282.

Baker, E.K., Harris, P.T., 1991. Copper, lead and zinc in the sediments of the Fly River Delta and Torres Strait. Mar. Pollut. Bull. 22 (12), 614–618.

Black, K.P., Oldman, J.W., 1999. Wave mechanisms responsible for grain sorting and non-uniform ripple distribution across two moderate-energy, sandy continental shelves. Mar. Geol. 162, 121–132.

Booij, N., Ris, C., Holthuijsen, L.H., 1999. A third-generation wave model for coastal regions 1. Model description and validation. J. Geophys. Res. 104, 7649–7666.

Bourg, A.C.M., 1987. Trace metal adsorption modelling and particle water interactions in estuarine environments. Cont. Shelf Res. 7, 1319–1332.

Church, J.A., Forbes, A.M.G., 1983. Circulation in the Gulf of Carpentaria: I. Direct observations of currents in the southeast corner of the Gulf of Carpentaria. Aust. J. Mar. Freshw. Res. 34, 1–10.

Clifton, H.E., Dingler, J.R., 1984. Wave formed structures and paleoenvironmental reconstruction. Mar. Geol. 60, 165–198.

Collins, L.B., 1988. Sediments and history of the Rottnest Shelf, southwest Australia: a swell dominated, non-tropical carbonate margin. Sediment. Geol. 60, 15–49.

Cook, P.J., Mayo, W., 1978. Sedimentology and Holocene history of a tropical estuary (Broad Sound, Queensland). Australian Bureau of Mineral Resources Bulletin, vol. 170. 206 pp.

Davies, P.J., 1979. Marine geology of the continental shelf off southeast Australia No. Bulletin 195). BMR, Bur. Miner. Resour. (51 pp.).

Easton, A.K., 1970. The tides of the continent of Australia. Research Report, vol. 37. Horace Lamb Centre for Oceanographic Research, Flinders University, South Australia. 326 pp.

Egbert, G.D., Bennett, A.F., Foreman, M.G.G., 1994. TOPEX/POSEIDON tides estimated using a global inverse model. J. Geophys. Res. 99, 24821–24852.

Freeland, H.J., Boland, F.M., Church, J.A., Clarke, A.J., Forbes, A.M.G., Huyer, A., Smith, R.L., Thompson, R.O.R.Y., White, N.J., 1986. The Australian coastal experiment: a search for coastal-trapped waves. J. Phys. Oceanogr. 16, 1230–1249.

Gagan, M.K., Chivas, A.R., Herczeg, A.L., 1990. Shelf wide erosion, deposition and suspended sediment transport during cyclone Winifred, central Great Barrier Reef, Australia. J. Sediment. Petrol. 60 (3), 456–470.

Gordon, A.D., Hoffman, J.G., 1986. Sediment features and processes of the Sydney continental shelf. In: Frankel, E., Keene, J.B., Waltho, A.E. (Eds.), Recent Sediments in Eastern Australia, Marine Through Terrestrial Sydney. Geological Society of Australia, NSW Division, pp. 29–52.

Grant, W.D., Madsen, O.S., 1979. Combined wave and current interaction with a rough bottom. J. Geophys. Res. 84 (C4), 1797–1808.

Grant, W.D., Madsen, O.S., 1986. The continental-shelf bottom boundary layer. Annu. Rev. Fluid Mech. 18, 265–305.

Gray, J.S., 1981. The ecology of marine sediments. Cambridge Studies in Modern Biology. Cambridge University Press, Cambridge. 185 pp.

Hammond, T.M., Collins, M.B., 1979. On the threshold of sand-sized sediment under the combined influence of unidirectional and oscillatory flow. Sedimentology 26, 795–812.

Harbison, P., 1984. Regional variation in the distribution of trace metals in modern intertidal sediments of northern Spencer Gulf, South Australia. Mar. Geol. 61, 221–247.

Hardisty, J., 1994. Beach and nearshore sediment transport. In: Pye, K. (Ed.), Sediment Transport and Depositional Processes. Blackwell, Oxford, pp. 219–255.

Harris, P.T., 1994. Comparison of tropical, carbonate and temperate, siliciclastic tidally dominated sedimentary deposits: examples from the Australian continental shelf. Aust. J. Earth Sci. 41, 241–254.

Harris, P.T., 1995. Marine geology and sedimentology of the Australian continental shelf. In: Zann, L.P., Kailola, P. (Eds.), The State of the Marine Environment Report for Australia Technical Annex 1: The Marine Environment Canberra, Department of the Environment, Sport and Territories, pp. 11–23.

Harris, P.T., Baker, E.K., 1991. The nature of sediments forming the Torres Strait turbidity maximum. Aust. J. Earth Sci. 38, 65–78.

Harris, P.T., Coleman, R., 1998. Estimating global shelf sediment mobility due to swell waves. Mar. Geol. 150, 171–177.

Harris, P.T., Baker, E.K., Cole, A.R., Short, S.A., 1993. A preliminary study of sedimentation in the tidally dominated Fly River Delta, Gulf of Papua. Cont. Shelf Res. 13 (4), 441–472.

Harris, P.T., Pattiaratchi, C.B., Collins, M.B., Dalrymple, R.W., 1995. What is a bedload parting?. In: Flemming, B.W., Bartholoma, A. (Eds.), Tidal Signatures in Modern and Ancient Environments. International Association of Sedimentologists Special Publication, vol. 24, pp. 1–18.

Harris, P.T., Tsuji, Y., Marshall, J.F., Davies, P.J., Honda, N., Matsuda, H., 1996. Sand and rhodolith-gravel entrainment on the mid- to outer-shelf under a western boundary current: Fraser Island continental shelf, eastern Australia. Mar. Geol. 129, 313–330.

Harris, P.T., Smith, R., Heggie, D., Heap, A., Bryce, S., Ryan, D., 2000. Classification of Australian estuaries based on wave, tide and river energy regime. Third International River Management Symposium, Brisbane, Qld., 6–8 Sept., 2000, 33.

Harris, P.T., Heap, A., Bryce, S., Smith, R., Ryan, D., Heggie, D., 2002. Classification of Australian clastic coastal depositional environments based upon a quantitative analysis of wave, tidal and fluvial power. J. Sediment. Res. 72 (6), 858–870.

Hasselman, K., WAMDI Group, 1988. The WAM model—a third generation ocean wave prediction model. J. Phys. Oceanogr. 18, 1775–1810.

Heap, A., 2000. Composition and dynamics of Holocene sediment next to the Whitsunday Islands on the middle shelf of the Great Barrier Reef platform, Australia. Unpublished PhD Thesis, James Cook University of North Queensland. 158 pp.

Hearn, C.J., Holloway, P.E., 1990. A three-dimensional barotropic model of the response of the Australian North West Shelf to tropical cyclones. J. Phys. Oceanogr. 20, 60–80.

James, N.P., Bone, Y., Von Der Borch, C.C., Gostin, V.A., 1992. Modern carbonate and terrigenous clastic sediments on a cool water, high energy mid-latitude shelf: Lacepede, southern Australia. Sedimentology 39, 877–903.

Jenkins, C.J., 2000. Generation of Seafloor Sediment Griddings for the UTAS-AGSO Shelf Sediment Mobility Project. Tech. Rep.—Ocean Sci. Inst. Univ. Syd. 89, 1–12.

Johnson, D.P., Searle, D.E., Hopley, D., 1982. Positive relief over buried post-glacial channels, Great Barrier Reef. Mar. Geol. 46, 149–159.

Jones, H.A., 1973. Marine geology of the northwest Australian continental shelf. Bur. Miner. Resour. Bull. 136 (Canberra).

Jones, H.A., Davies, P.J., 1983. Superficial sediments of the Tasmanian continental shelf and part of Bass Strait. Bur. Miner. Resour. Bull. 218 (Canberra).

Jones, H.A., Kudras, H.R., 1982. SONNE SO-15 cruise 1980 off the east coast of Australia—bathymetry and seafloor morphology. Geol. Jahrb., Reihe D D56, 55–67.

Kailola, P.J., Williams, M.J., Stewart, P.C., Reichelt, R.E., McNee, A., Grieve, C., 1993. Australian Fisheries Resources. Bureau of Rural Resources, Canberra, ACT. 422 pp.

Kantha, L.H., 1995. Barotropic tides in the global oceans from a nonlinear tidal model assimilating altimetric tides 1. Model description and results. J. Geophys Res. 100 (C12), 25283–25308.

Komar, P.D., Miller, M.C., 1973. The threshold of sediment movement under oscillatory water waves. J. Sediment. Petrol. 43, 1101–1110.

Komen, G., Cavaleri, L., Donelan, M., Hasselman, K., Hasselman, S., Janssen, P.A.E.M., 1994. Dynamics and Modelling of Ocean Waves. Cambridge University Press, Cambridge. 532 pp.

Kostylev, V.E., Todd, B.J., Fader, G.B.J., Courtney, R.C., Cameron, G.D.M., Pickrill, R.A., 2000. Benthic habitat mapping on the Scotian Shelf based on multibeam bathymetry, surficial geology and sea floor photographs. Mar. Ecol., Prog. Ser. 219, 121–134.

Long, B.G., Poiner, I.R., Wassenberg, T.J., 1995. Distribution, biomass and community structure of megabenthos of the Gulf of Carpentaria, Australia. Mar. Ecol., Prog. Ser. 129, 127–139.

Louis, J.P., Radok, J.R.M., 1975. Propagation of tidal waves in the Joseph Bonaparte Gulf. J. Geophys. Res. 80 (12), 1689–1690.

Lourensz, R.S., 1981. Tropical Cyclones in the Australian Region July 1909 to June 1980, 2nd ed. Hedges and Bell Publ., Maryborough, Victoria.

Lyne, V.D., Butman, B., Grant, W.D., 1990. Sediment movement along the U.S. east coast continental shelf: I. Estimates of bottom stress using the Grant–Madsen model and near-bottom wave and current measurements. Cont. Shelf Res. 10, 397–428.

Madsen, O.S., 1994. Spectral wave-current bottom boundary layer flows. Proceedings of the 24th International Conference on Coastal Engineering, Coastal Engineering Research Council/ ASCE, Kobe, Japan, pp. 384–398.

McMillan, J.D., 1982. A Global Atlas of GEOS-3 Significant Waveheight Data and Comparison of the Data with National Buoy Data No. 156882. NASA, Wallops Flight Center, Virginia.

Miller, M.C., McCave, I.N., Komar, P.D., 1977. Threshold of sediment motion under unidirectional currents. Sedimentology 24, 507–527.

Pattiaratchi, C.B., Collins, M.B., 1985. Sand transport under the combined influence of waves and tidal currents: an assessment of available formulae. Mar. Geol. 67, 83–100.

Pearce, A.F., Pattiaratchi, C.B., 1997. Applications of satellite remote sensing to the marine environment in Western Australia. J. R. Soc. West. Aust. 80, 1–14.

Phillips, D.M., Scholtz, M.L., 1982. Measured distribution of water turbidity in Gulf St. Vincent. Aust. J. Mar. Freshw. Res. 33, 723–737.

Pingree, R.D., Griffiths, D.K., 1979. Sand tranport paths around the British Isles resulting from M2 and M4 tidal interactions. J. Mar. Biol. Assoc. UK 59, 497–513.

Poiner, I.R., Kennedy, R., 1984. Complex patterns of change in the macrobenthos of a large sandbank following dredging. Mar. Biol. 78 (3), 335–352.

Semeniuk, V., 1982. Geomorphology and Holocene history of the tidal flats, King Sound, north-western Australia. J. R. Soc. West. Aust. 65 (2), 47–68.

Shepherd, S.A., 1983. Benthic communities of upper Spencer Gulf, South Australia. Trans. Royal Soc. S. Aust. 107 (2), 69–85.

Shum, C.K., Woodworth, P.L., Andersen, O.B., Egbert, G., Francis, O., King, C., Klosko, S., Le Provost, C., Li, X., Molines, J., Parke, M., Ray, R., Schlax, M., Stammer, D., Tierney, C., Vincent, P., Wunch, C., 1997. Accuracy assessment of recent ocean tide models. J. Geophys. Res. 102 (C11), 25.173.

Smith, W.H., Sandwell, D.T., 1997. Global sea floor topography from satellite altimetry and ship depth soundings. Sci. Mag. 277 (5334).

Somers, I.F., 1987. Sediment type as a factor in the distribution of commercial prawn species in the western Gulf of Carpentaria, Australia. Aust. J. Mar. Freshw. Res. 38, 133–149.

Swift, D.J.P., Thorne, J.A., 1991. Sedimentation on continental margins: I. A general model for shelf sedimentation. Spec. Publ. Int. Assoc. Sedimentol. 14, 3–31.

Swift, D.J.P., Stanley, D.J., Curray, J.R., 1971. Relict sediments, a reconsideration. J. Geol. 79, 322–346.

Swift, D.J.P., Han, G., Vincent, C.E., 1986. Fluid processes and sea-floor response on a modern storm-dominated shelf: Middle Atlantic shelf of north America: Part 1. The storm-current regime. In: Knight, R.J., McLean, J.R. (Eds.), Shelf Sands and Sandstones. Canadian Society of Petroleum Geologists, Calgary, pp. 99–119.

Todd, B.J., Kostylev, V.E., Fader, G.B.J., Courtney, R.C., Pickerill, R.A., 2000. New approaches to benthic mapping integrating multibeam bathymetry and backscatter, surficial geology and sea floor photographs: A case study from the Scotian shelf, Atlantic Canada. ICES 2000 Annual Science Conference 27–30 September Bruges, Belgium.

Vincent, C.E., 1986. Processes affecting sand transport on a storm-dominated shelf. In: Knight, R.J., McLean, J.R. (Eds.), Shelf Sands and Sandstones Calgary. Canadian Society of Petroleum Geologists, pp. 121–132.

Walker, R.G., 1984. Shelf and shallow marine sands. In: Walker, R.G. (Ed.), Facies Models. Geological Association of Canada, Toronto, pp. 141–170.

Wolanski, E., 1985. Some properties of waves at the Queensland shelf break. 7th Australasian Conference on Coastal and Ocean Engineering, vol. 2, pp. 61–70. Christchurch, NZ.